JOURNAL OF COMPUTATIONAL PHYSICS 103, 402–414 (1992)

Resolution of the 2D Navier–Stokes Equations in Velocity–Vorticity Form by Means of an Influence Matrix Technique

O. DAUBE

LIMSI-CNRS, BP 133, 91403 Orsay Cedex, France

Received October 16, 1990; revised November 11, 1991

An influence matrix technique is proposed to enforce both the continuity equation and the definition of the vorticity in the treatment of the 2D incompressible Navier–Stokes equations. It is shown and supported by numerical experiments that at each time step the divergence is actually equal to zero within machine accuracy. The same result is obtained for the definition of the vorticity.

1. INTRODUCTION

The vorticity–velocity formulation of the Navier–Stokes equations is very familiar to people working in the field of vortex or/and particle methods but is less popular in the context of methods involving grids (finite differences, finite elements, ...) despite the fact that it has been used for more than 10 years [3, 4]. It seems, however, that this formulation is, to a growing number of people, an attractive alternative to formulations in primitive variables or in terms of the vorticity and of a vector potential for the resolution of the 3D Navier–Stokes equations. This interest is due to several reasons [1, 2], but it seems that the main one is linked to easier treatment of the boundary conditions since the pressure is no longer part of the resolution. One may also say that this formulation is closer to physical reality, especially in the case of vortex dominated flows [5] and that, in the case of external flows, conditions at infinity are easier to implement than those for the pressure. Another desirable feature is that this formulation is valid in both two and three dimensions.

A real interest in this formulation has grown recently owing to the increasing power of computers which permits tackling 3D flows. During this period, the need of an efficient alternative to the formulation using the primitive variables of the Navier–Stokes equations was felt increasingly necessary. Most of the studies using the vorticity–velocity formulation have been concerned with internal incompressible 2D or 3D flows [3–8, 12, 13] but applications to external flows or to semi-bounded flows can also be found [7, 9, 11]. Recently, additional characteristics of the fluid such as compressibility, have been taken into account [2].

The set of equations to be solved always includes a vorticity transport equation which is derived by taking the curl of the momentum equation. Concerning the remaining equations, two alternative approaches may be considered:

(1) Solve the continuity and the vorticity definition equations.

(2) Solve Poisson equations for the components of the velocity.

Among the previous authors, only Gatski *et al.* [6, 7] and Osswald *et al.* [5] used the first approach, whereas in all the other studies Poisson equations were used. As noted, for instance, by [9], the major problem that arises when using the formulation with Poisson equations is the satisfaction of the continuity equation. In this paper, that is restricted to 2D flows, it is shown that satisfying the continuity equation is equivalent to enforcing the definition of the vorticity as the curl of the velocity field and that these requirements reduce to boundary conditions coupling the velocity and the vorticity or the divergence. This fact was already pointed out by Cottet [10] in the context of vortex methods.

To overcome the difficulties involved by this coupling at the boundaries, two influence matrix techniques are presented. The influence matrix technique, also known as the capacitance matrix technique, has been widely used to solve systems of elliptic linear equations for which either the domain of integration has irregular boundaries [15 18], or boundary conditions are not available for all the unknowns despite theorems proving existence and uniqueness [19], or to solve elliptic vector problems with coupled boundary conditions for the components [27]. In all cases, the technique makes use of the principle of superposition of solutions to elementary problems. A linear combination of these elementary solutions is then sought in order to ensure

0021-9991/92 $5.00

additional conditions which are not taken into account in the elementary problems but have to be fullfilled to obtain a solution to the initial problem. All these techniques may be seen as applications of numerical Green's functions.

Kleiser and Schumann [19] were apparently the first to use the influence matrix technique for solving the incompressible Navier–Stokes equations in primitive variables. Their work was restricted to 3D flows with two directions of periodicity and it used a spectral Fourier–Tchebychev method. Later, this technique was extended by LeQuéré and Alziary de Roquefort [20; 21] to 2D problems without periodicity, using Tchebychev expansions in both directions. In these studies, the incompressibility constraint is ensured by expressing a linear relationship between a trial distribution of pressure along the boundary and the value of the divergence along the same boundary. A generalization of this technique, especially in cylindrical coordinates, can be found in Tuckerman [22].

In addition to these studies in which the Navier–Stokes equations were cast in primitive variables, the influence matrix technique was also used to overcome the lack of boundary conditions for ω, when solving 2D or axisymmetric Navier–Stokes equations formulated in terms of the stream function Ψ and of the vorticity function ω [23–25]. In this case, the influence matrix expresses a linear relationship between the distribution of vorticity and tangential velocity along the boundaries. The advantage is that a strong coupling at the same time level between Ψ and ω is obtained which is lacking in the usual methods, where a time shift has to be introduced at the boundaries in order to decouple the equations.

It is important to note that the Kleiser and Schumann method was found to be equivalent to the integral conditions for the pressure which have been established by Quartapelle and Napolitano [26] and Quartapelle [28] and which may be considered to some extent as an extension to Navier–Stokes problems of the method of Glowinski and Pironneau [29] which was originally designed for Stokes flows.

One common feature of these techniques is that at each time level $n\,\Delta t$, the boundary values of the unknowns (pressure or vorticity) are computed through the multiplication of a N_Γ vector by a *dense* $N_\Gamma \times N_\Gamma$ matrix, where N_Γ denotes the number of boundary nodes involved in the discretization process. This matrix does not depend upon the time level and can therefore be computed and inverted in a preprocessing stage.

In this paper, two influence matrix methods are proposed to solve the 2D incompressible Navier–Stokes equations in vorticity–velocity formulation. They are designed to make sure that both the continuity equation $\nabla \cdot \mathbf{v} = 0$ and the definition of the vorticity function $\nabla \times \mathbf{v} = \omega \mathbf{k}$ are satisfied at the same time level. This strong coupling between the velocity and the vorticity which is not found in most of the previous studies and which is particularly important in the case of unsteady flows, formally maintains the temporal accuracy of the time discretization. The basic numerical method is a standard second-order finite difference scheme using a regular staggered MAC grid. Numerical evidence of the efficiency of the present method is supported by the resolution of two flows: the driven square cavity and the axisymmetric flow in a cylindrical container with a rotating lid. In both cases, the results are in good agreement with the previously known results and the divergence field is actually shown to be zero within machine accuracy.

2. THE VORTICITY–VELOCITY FORMULATION

This paper is restricted to the case of a bounded simply connected domain $\mathscr{D}$ with boundary Γ. The additional problems that arise when considering multiply connected domains are adressed in Daube *et al.* [14]. Taking the curl of the momentum equation and taking into account the continuity equation yields

$$\frac{\partial \omega}{\partial t} + \nabla \cdot (\omega \mathbf{v}) = \frac{1}{\mathrm{Re}} \nabla^2 \omega \qquad \text{in } \mathscr{D} \tag{1}$$

$$\nabla \times \mathbf{v} = \omega \mathbf{k} \qquad \text{in } \mathscr{D} \tag{2}$$

$$\nabla \cdot \mathbf{v} = 0 \qquad \text{in } \mathscr{D} \tag{3}$$

$$\mathbf{v} = \mathbf{v}_\Gamma \qquad \text{on } \Gamma = \partial \mathscr{D}; \tag{4}$$

$\mathbf{v}$ must also satisfy a compatibility relation,

$$\int_\Gamma \mathbf{v} \cdot \mathbf{n}\, d\sigma = 0, \tag{5}$$

where $\mathbf{v}$ is the velocity vector, ω is the vorticity function, and Re is the Reynolds number. The vector $\mathbf{k}$ is a unit vector normal to the plane of the flow and $\mathbf{n}$ is a unit vector normal to the boundary Γ. In addition, the initial conditions must satisfy (2)–(5). Equation (2) is often replaced by a second-order equation which is obtained by using the well-known vector relation defining the vector laplacian,

$$\nabla^2 \mathbf{f} = \nabla(\nabla \cdot \mathbf{f}) - \nabla \times (\nabla \times \mathbf{f}) \tag{6}$$

that is valid for any vector field $\mathbf{f}$. Using (6) in conjunction with the continuity equation (3) yields

$$\nabla^2 \mathbf{v} = -\nabla \times (\omega \mathbf{k}) = \mathbf{k} \times \nabla \omega. \tag{7}$$

Equations (1) and (7) with boundary conditions (4) are not equivalent to the original system (1 to 4) and the major difficulty arises from this point. In fact, additional conditions have to be written in order to satisfy Eqs. (3) and (2) everywhere. This point will be made clearer in the next sections.

3. TEMPORAL DISCRETIZATION

As usual with the influence matrix techniques, a semi-implicit scheme has to be used to advance the solution in time. To this end the classical Adams–Bashforth–Crank–Nicolson (ABCN) scheme was chosen. It consists in writing the transport equation (1) at the time level $(n+\frac{1}{2})\,\Delta t$ and evaluating the diffusion terms implicitly and the convective terms explicitly at this time level by means of an Adams–Bashforth extrapolation. At each time step, a Helmholtz equation has to be solved, together with the continuity equation and the vorticity definition. More precisely, the following system is obtained, where the superscripts denote the time levels at which the variables are considered and I is the identity operator:

$$\begin{aligned}
(\sigma \mathrm{I} - \nabla^2)\,\omega^{(n+1)} &= S^{(n)} && \text{in } \mathscr{D} \\
\nabla \times \mathbf{v}^{(n+1)} &= \omega^{(n+1)}\mathbf{k} && \text{in } \mathscr{D} \\
\nabla \cdot \mathbf{v}^{(n+1)} &= 0 && \text{in } \mathscr{D} \qquad (8) \\
\mathbf{v}^{(n+1)} &= \mathbf{v}_\Gamma && \text{on } \Gamma \\
\int_\Gamma \mathbf{v}^{n+1} \cdot \mathbf{n}\, d\sigma &= 0.
\end{aligned}$$

The use of a semi-implicit time discretization always leads to a system of the form (8). In the particular case of the ABCN scheme, we have

$$\sigma = \frac{2\mathrm{Re}}{\Delta t};$$

$$S^{(n)} = (\sigma \mathrm{I} + \nabla^2)\,\omega^{(n)} - \mathrm{Re}(3\nabla \cdot (\omega \mathbf{v})^{(n)} - \nabla \cdot (\omega \mathbf{v})^{(n-1)}).$$

Remark. Throughout the paper, we will assume the existence and uniqueness of the solutions of system (8).

4. THE LAPLACIAN OF THE VELOCITY

In order to solve second-order elliptic equations, we introduce the relation (7) into the system (8) in place of one or both Eqs. (3) and (2). In doing so, we have to make sure that the resulting set of equations is equivalent to the original system. This section is devoted to this point.

With this in mind consider some solution $(\mathbf{v}, \omega)$ of the system:

$$\begin{aligned}
(\sigma \mathrm{I} - \nabla^2)\omega &= S && \text{in } \mathscr{D} \\
\nabla^2 \mathbf{v} &= \mathbf{k} \times \nabla\omega && \text{in } \mathscr{D} \qquad (9) \\
\mathbf{v} &= \mathbf{v}_\Gamma && \text{on } \Gamma.
\end{aligned}$$

Concerning this system, it must be noticed that:

(1) It has an infinite number of solutions.

(2) The solution of the original problem (8) is obviously a solution of (9).

(3) The function ω is not necessarily the vorticity of the vector field $\mathbf{v}$.

(4) The divergence of $\mathbf{v}$ is not necessarily equal to 0.

We now establish the propositions—that can be in part found in Cottet [10]—which constitute the foundations of the influence matrix techniques that we propose and that rely upon a linear relationship between the distribution of ω on the boundary and the values of either the divergence $\nabla \cdot \mathbf{v}$ or $(\nabla \times \mathbf{v}) \cdot \mathbf{k} - \omega$ on this boundary.

4.1. *Enforcing the Continuity Equation*

PROPOSITION 1. *A necessary and sufficient condition for a solution* $(\mathbf{v}, \omega)$ *of* (9) *to satisfy the additional condition* $\nabla \cdot \mathbf{v} = 0$ *in* $\mathscr{D}$ *is*

$$\nabla \cdot \mathbf{v} = 0 \qquad \text{on} \quad \Gamma = \partial\mathscr{D}. \qquad (10)$$

Proof. Let $(\mathbf{v}, \omega)$ be a solution of (9). From relation (7) it follows that

$$\nabla(\nabla \cdot \mathbf{v}) = -\nabla \times (\omega \mathbf{k} - \nabla \times \mathbf{v})$$

the divergence of which yields

$$\nabla^2(\nabla \cdot \mathbf{v}) = 0 \qquad \text{in } \mathscr{D}.$$

The scalar function $\nabla \cdot \mathbf{v}$ is thus a solution of the Laplace equation. Therefore, a necessary and sufficient condition for the divergence of the velocity to be zero everywhere is that it vanishes on the boundary, i.e., relation (10) be satisfied. ∎

PROPOSITION 2. *Let* $(\mathbf{v}, \omega)$ *be a solution of* (9) *which satisfies* (10) (*recall that* $\omega\mathbf{k}$ *is not necessarily the curl of* $\mathbf{v}$). *Defining* ζ *by* $\nabla \times \mathbf{v} = \zeta \mathbf{k}$, *the following relation holds*:

$$\zeta - \omega = \textit{constant in } \mathscr{D}$$

Proof. The definition for ζ with the relations (6) and (7) yields

$$\nabla^2 \mathbf{v} = \nabla(\nabla \cdot \mathbf{v}) + \mathbf{k} \times \nabla\zeta = \mathbf{k} \times \nabla\omega.$$

Since $\mathbf{v}$ satisfies the continuity equation it follows that $\nabla(\zeta - \omega) = 0$ in $\mathscr{D}$, which proves the proposition. ∎

Propositions 1 and 2 have the following immediate consequence:

COROLLARY 3. *The initial problem* (8) *is equivalent to the following one*:

$$\begin{aligned}(\sigma \mathrm{I}-\nabla^2)\omega &= S && \text{in } \mathscr{D}\\ \nabla^2 \mathbf{v} &= \mathbf{k}\times\nabla\omega && \text{in } \mathscr{D}\\ \mathbf{v} &= \mathbf{v}_\Gamma && \text{on } \Gamma\\ \nabla\cdot\mathbf{v} &= 0 && \text{on } \Gamma\\ \zeta &= \omega && \text{at one point of } \mathscr{D}.\end{aligned} \tag{11}$$

4.2. *Enforcing the Definition of the Vorticity*

PROPOSITION 4. *Let* ζ *be defined by* $\nabla\times\mathbf{v}=\zeta\mathbf{k}$. *A necessary and sufficient condition for a solution* $(\mathbf{v}, \omega)$ *of the system* (9) *to satisfy the additional condition* $\zeta=\omega$ *in* $\mathscr{D}$ *is*

$$\zeta=\omega \qquad \text{on} \quad \Gamma=\partial\mathscr{D}. \tag{12}$$

Proof. Since $(\mathbf{v}, \omega)$ is a solution of (9) we have

$$\nabla^2\mathbf{v}=\nabla(\nabla\cdot\mathbf{v})+\mathbf{k}\times\nabla\zeta=\mathbf{k}\times\nabla\omega,$$

the cross product of which with $\mathbf{k}$ yields

$$\mathbf{k}\times\nabla(\nabla\cdot\mathbf{v})=-\nabla(\zeta-\omega)$$

and, taking the divergence, leads to

$$\nabla^2(\zeta-\omega)=0 \qquad \text{in } \mathscr{D}.$$

The difference $(\zeta-\omega)$ satisfies the Laplace equation. Therefore, the condition (12) is necessary and sufficient to ensure that ω is the vorticity function of the velocity field $\mathbf{v}$. ∎

PROPOSITION 5. *Let* $(\mathbf{v}, \omega)$ *be a solution of* (9) *which satisfies* (12). *Then, the velocity field* $\mathbf{v}$ *is divergence free*:

$$\nabla\cdot\mathbf{v}=0 \qquad \text{in } \mathscr{D}.$$

Proof. The function ω is the vorticity of the velocity field $\mathbf{v}$. From the definition of the laplacian vector (6), it follows that $\nabla(\nabla\cdot\mathbf{v})=0$ in $\mathscr{D}$, i.e., $\nabla\cdot\mathbf{v}$ is constant in $\mathscr{D}$. From the compatibility relation (5) it follows that this constant is equal to zero. ∎

Propositions (4) and (5) have the following immediate consequence:

COROLLARY 6. *The initial problem* (8) *is equivalent to the following one*:

$$\begin{aligned}(\sigma \mathrm{I}-\nabla^2)\omega &= S && \text{in } \mathscr{D}\\ \nabla^2 \mathbf{v} &= \mathbf{k}\times\nabla\omega && \text{in } \mathscr{D}\\ \mathbf{v} &= \mathbf{v}_\Gamma && \text{on } \Gamma\\ \nabla\times\mathbf{v} &= \omega\mathbf{k} && \text{on} \quad \Gamma=\partial\mathscr{D}.\end{aligned} \tag{13}$$

5. THE INFLUENCE MATRIX METHOD

5.1. *The Superposition Principle*

As mentioned in the Introduction, the influence matrix method makes use of the superposition principle for linear problems. We are now going to split the initial problem (8) into several linear problems that we are able to solve without major difficulties. First, let ω_Γ be a given function on Γ and let us consider the problem [A] defined as follows: Find $(\tilde{\mathbf{v}}, \tilde{\omega})$ which satisfy:

$$[\mathrm{A}]\begin{cases}(\sigma \mathrm{I}-\nabla^2)\tilde{\omega}=S & \text{in } \mathscr{D}\\ \tilde{\omega}=\omega_\Gamma & \text{on } \Gamma\\ \nabla^2\tilde{\mathbf{v}}=\mathbf{k}\times\nabla\tilde{\omega} & \text{in } \mathscr{D}\\ \tilde{\mathbf{v}}=\mathbf{v}_\Gamma & \text{on } \Gamma.\end{cases}$$

The problem [A] clearly has a unique solution for a given distribution ω_Γ. Let $(\mathbf{v}, \omega)$ be the unique solution of the original problem (8) and let $(\hat{\mathbf{v}}, \hat{\omega})$ be the difference $(\tilde{\mathbf{v}}-\mathbf{v}, \tilde{\omega}-\omega)$. Owing to the linearity of the considered problems, $(\hat{\mathbf{v}}, \hat{\omega})$ is a solution of the homogeneous system:

$$\begin{aligned}(\sigma \mathrm{I}-\nabla^2)\hat{\omega} &= 0 && \text{in } \mathscr{D}\\ \nabla^2\hat{\mathbf{v}} &= \mathbf{k}\times\nabla\hat{\omega} && \text{in } \mathscr{D}\\ \hat{\mathbf{v}} &= 0 && \text{on } \Gamma.\end{aligned} \tag{14}$$

Let us assume that a set of discretization points over the domain $\mathscr{D}$ has been defined and let N_Γ be the number of such points which lie along the boundaries. The solutions of (14) are then fully determined by the distribution of $\hat{\omega}$ on the N_Γ boundary nodes. They belong to the space spanned by the solutions $(\hat{\mathbf{v}}_k, \hat{\omega}_k)$ of the elementary problems $[B_k]$ $(k=1, ..., N_\Gamma)$ defined by

$$[\mathrm{B}_k]\begin{cases}(\sigma \mathrm{I}-\nabla^2)\hat{\omega}_k=0 & \text{in } \mathscr{D}\\ \hat{\omega}_k(\gamma_j)=\delta_{kj} & \forall\gamma_j\in\Gamma\\ \nabla^2\hat{\mathbf{v}}_k=\mathbf{k}\times\nabla\hat{\omega}_k & \text{in } \mathscr{D}\\ \hat{\mathbf{v}}_k=0 & \text{on } \Gamma,\end{cases}$$

where δ_{kj} is the Kronecker symbol. Each of these problems clearly has a unique solution which does not depend upon the actual time level (n) and should therefore be solved in a preprocessing stage.

By virtue of the superposition principle, the solution $(\mathbf{v}, \omega)$ of the problem (8) is sought as a linear combination of $(\tilde{\mathbf{v}}, \tilde{\omega})$ and of the $(\hat{\mathbf{v}}_k, \hat{\omega}_k)$:

$$\mathbf{v}=\tilde{\mathbf{v}}+\sum_{k=1}^{k=N_\Gamma}\lambda_k\hat{\mathbf{v}}_k$$

$$\omega=\tilde{\omega}+\sum_{k=1}^{k=N_\Gamma}\lambda_k\hat{\omega}_k.$$

Because of the definition of the functions $\hat{\omega}_k$, the coefficients $\{\lambda_k\}_{k=1,...,N_\Gamma}$ are related to the actual values of the vorticity ω on the boundary Γ by

$$\omega(\gamma_k) = \tilde{\omega}(\gamma_k) + \lambda_k = \omega_\Gamma(\gamma_k) + \lambda_k, \qquad \forall \gamma_k \in \Gamma. \quad (15)$$

The remaining task is to determine these coefficients in order to ensure that the conditions that are not yet taken into account, i.e., the continuity equation and the vorticity definition, are satisfied.

5.2. *Building of the Influence Matrix*

At this point, we can use either corollary (3) or corollary (6) which would lead to two different matrices. We present here the matrix obtained by choosing corollary (6) which is the one that can be readily extended to the three-dimensional case.

The coefficients λ_k are computed in order to ensure that the definition of the vorticity (2) is satisfied at the N_Γ discretization points M_i that are located on the boundary Γ,

$$(\bar{\zeta} - \tilde{\omega})(M_i) + \sum_{k=1}^{k=N_\Gamma} \lambda_k (\hat{\zeta}_k - \hat{\omega}_k)(M_i) = 0, \qquad \forall i = 1, ..., N_\Gamma, \quad (16)$$

where $\bar{\zeta}$ (resp. $\hat{\zeta}_k$) is defined by

$$\nabla \times \bar{\mathbf{v}} \text{ (resp. } \hat{\mathbf{v}}_k) = \bar{\zeta}\mathbf{k} \text{ (resp. } \hat{\zeta}_k \mathbf{k}).$$

Equations (16) can be cast in matrix form:

$$\mathbf{A} \cdot \boldsymbol{\lambda} = \mathbf{f}.$$

The elements a_{ij} of the matrix $\mathbf{A}$ of order N_Γ are defined by

$$a_{ik} = (\hat{\zeta}_k - \hat{\omega}_k)(M_i), \qquad i = 1, ..., N_\Gamma; k = 1, ..., N_\Gamma$$

and the elements f_i of the vector $\mathbf{f}$ are defined by

$$f_i = -(\bar{\zeta} - \tilde{\omega})(M_i), \qquad i = 1, ..., N_\Gamma.$$

Provided that the unknowns are considered in the right functional spaces, the invertibility of the matrix $\mathbf{A}$ derives from the uniqueness of the solution of problem (8) (see Section 9). The unknown vector $\boldsymbol{\lambda}$ is then obtained as

$$\boldsymbol{\lambda} = \mathbf{A}^{-1} \cdot \mathbf{f}.$$

The inverse of matrix $\mathbf{A}$ is computed in a preprocessing stage. At each time step, the multiplication of a N_Γ vector by a matrix of order N_Γ is required to obtain the vector $\boldsymbol{\lambda}$.

Because it is more economical to twice solve system [A] than to keep in central core all the $(\hat{\mathbf{v}}_k, \hat{\omega}_k)$ in order to achieve adequate linear combinations, the computations for one time step Δt are performed in the following way:

(1) Compute the solution of problem [A] with a given distribution of $\tilde{\omega}$ on the boundary (for instance, the values of ω at the previous time step, or everywhere 0).

(2) Compute the difference $\bar{\zeta} - \tilde{\omega}$ at the control points M_i.

(3) Compute the coefficients λ_k by multiplying these values by $\mathbf{A}^{-1}$ and obtain the true values of the vorticity along the boundaries by means of the relation (15).

(4) Again solve problem [A] with the true boundary values of the vorticity.

The calculation of one time step requires the solution of six elliptic equations which will be solved by means of a fast elliptic solver (see next section).

5.3. *Another Influence Matrix*

In the previous section the influence matrix has been built to enforce the definition of the vorticity at every point of $\mathscr{D}$. From corollary (3) another influence matrix can be built in order to enforce the zero divergence at $N_\Gamma - 1$ points M_i of the boundary and the definition of the vorticity at one arbitrary point P of $\mathscr{D}$. The computational process will thus be essentially the same as the one previously described. With the same notations as in Section 5.2 the influence matrix $\mathbf{A}$ is defined as

$$a_{ik} = (\nabla \cdot \hat{\mathbf{v}}_k)(M_i), \qquad i = 1, ..., N_\Gamma - 1; k = 1, ..., N_\Gamma$$
$$a_{N_\Gamma, k} = (\hat{\zeta}_k - \hat{\omega}_k)(P), \qquad k = 1, ..., N_\Gamma,$$

and the elements f_i of the source vector $\mathbf{f}$ are defined by

$$f_i = -(\nabla \cdot \tilde{\mathbf{v}})(M_i), \qquad i = 1, ..., N_\Gamma - 1,$$
$$f_{N_\Gamma} = -(\bar{\zeta} - \tilde{\omega})(P).$$

It will be shown in the section on results that these two techniques give equivalent results within machine accuracy.

6. NUMERICAL IMPLEMENTATION

6.1. *The Spatial Discretization*

For the sake of simplicity, we assume that the domain $\mathscr{D}$ is rectangular and is divided in $M \times N$ regular meshes. The spatial discretization steps are then:

$$\Delta x = \frac{1}{M}; \qquad \Delta y = \frac{1}{N}.$$

To ensure that the unknown discrete functions belong to the right functional spaces, a staggered MAC grid is used.

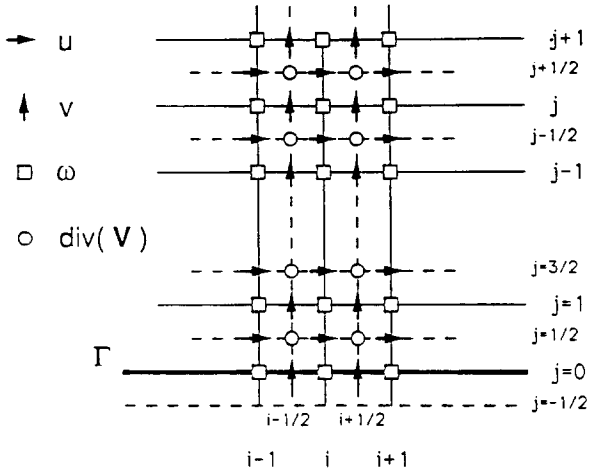

FIG. 1. The MAC grid.

Standard second-order centered differences have been used for both first and second derivatives. The collocation points for the different unknown functions are defined (see Fig. 1) as follows:

- The velocity component u is computed at nodes $(i\,\Delta x, (j+\frac{1}{2})\,\Delta y)$ for $i=0, ..., M$ and $j=0, ..., N-1$.
- The velocity component v is computed at nodes $((i+\frac{1}{2})\,\Delta x, j\,\Delta y)$ for $i=0, ..., M-1$ and $j=0, ..., N$.
- The vorticity ω is computed at nodes $(i\,\Delta x, j\,\Delta y)$ for $i=0, ..., M$ and $j=0, ..., N$:

$$\omega_{ij}=\frac{v_{i+1/2,j}-v_{i-1/2,j}}{\Delta x}-\frac{u_{i,j+1/2}-u_{i,j-1/2}}{\Delta y}.$$

- The divergence $\nabla\cdot\mathbf{v}$ is computed at the center of the meshes: $((i+\frac{1}{2})\,\Delta x,\ (j+\frac{1}{2})\,\Delta y)$ for $i=0, ..., M-1$ and $j=0, ..., N-1$:

$$(\nabla\cdot\mathbf{v})_{i+1/2,j+1/2}=\frac{u_{i+1,j+1/2}-u_{i,j+1/2}}{\Delta x}+\frac{v_{i+1/2,j+1}-v_{i+1/2,j}}{\Delta y}.$$

6.2. *Resolution of the Helmholtz Equation*

The only sensitive point in this resolution is the calculation of the convective terms because it makes use of the components of the velocity at points where they are not computed. For instance, let us consider the approximation of $\partial(u\omega)/\partial x$ by the following finite difference:

$$\frac{\partial}{\partial x}(u\omega)_{ij}\simeq\frac{\bar{u}_{i+1/2,j}\omega_{i+1/2,j}-\bar{u}_{i-1/2,j}\omega_{i-1/2,j}}{\Delta x}.$$

The points $(i+\frac{1}{2}, j)$ and $(i-\frac{1}{2}, j)$ are not collocation points for the u-component of the velocity. Therefore the approximations $\bar{u}$ are obtained by a bilinear interpolation on the values of u at the four nodes that are the immediate neighbours of the node $(i+\frac{1}{2}, j)$. In our case, owing to the regular mesh, this interpolation reduces to the arithmetic mean:

$$\bar{u}_{i+1/2,j}=\tfrac{1}{4}(u_{i,j-1/2}+u_{i,j+1/2}+u_{i+1,j-1/2}+u_{i+1,j+1/2}).$$

For similar reasons, $\omega_{i+1/2,j}$ is defined as the mean value:

$$\omega_{i+1/2,j}=\tfrac{1}{2}(\omega_{ij}+\omega_{i+1,j}).$$

6.3. *Discretization of the u-Equation*

- In the x-direction, the standard second-order centered difference can be used at each interior point in $\mathscr{D}$, since there are collocation points for u on the vertical boundaries $x=0$ and $x=1$:

$$\left(\frac{\partial^2 u}{\partial x^2}\right)_{ij}\simeq\delta_{xx}u_{ij}=\frac{1}{\Delta x^2}(u_{i-1,j}-2u_{ij}+u_{i+1,j}).$$

- In the y-direction, standard second-order centered differences can be used at each interior point which is not adjacent to horizontal boundary:

$$\left(\frac{\partial^2 u}{\partial y^2}\right)_{ij}\simeq\delta_{yy}u_{ij}=\frac{1}{\Delta y^2}(u_{i,j-1}-2u_{ij}+u_{i,j+1}).$$

On the nodes adjacent to the horizontal boundaries $y=0$, the second derivative of u with respect to y is approximated by the difference:

$$\left(\frac{\partial^2 u}{\partial y^2}\right)_{i,1/2}=\frac{4}{3\Delta y^2}(u_{i,3/2}-3u_{i,1/2}+2u_{i,0}).$$

This approximation is in fact (see [30]) the usual centered difference over the points $(i, -\frac{1}{2})$, $(i, \frac{1}{2})$, and $(i, \frac{3}{2})$ in which the value of u at the fictitious point $(i, -\frac{1}{2})$ outside the domain (see Fig. 1) is calculated by the extrapolation:

$$u_{i,-1/2}=\tfrac{1}{3}(u_{i,3/2}-6u_{i,1/2}+8u_{i,0}).$$

- The y-derivative of u on the boundary $y=0$, i.e., the vorticity, is computed by using the extrapolated value for $u_{i,-1/2}$, yielding

$$\left(\frac{\partial u}{\partial y}\right)_{i,0}=\frac{1}{3\Delta y}(-u_{i,3/2}+9u_{i,1/2}-8u_{i,0}).$$

6.4. *Resolution of the Discretized Problems*

Fast direct solvers have been used throughout this work, taking advantage of the separability of the equations for the

considered problems. They are called Fourier–Toeplitz methods in the literature [31, 32]. For instance, in the case of the u-component, the discretized equations are written in the tensor product basis $\{\phi_i \otimes \mathbf{e}_j\}_{i=1,\ldots,M-1}^{j=0,\ldots,N}$, where $\{\phi_i\}$ is the basis of eigenvectors of the second centered difference δ_{xx} and $\{\mathbf{e}_j\}$ the canonical basis in the y-direction. This change of basis is performed through a FFT for large enough values of M and by matrix multiplication otherwise. Obtaining the solution in the tensor product basis then requires the resolution of N tridiagonal systems and an inverse FFT (or matrix multiplication) gives the results in physical space.

7. THE DRIVEN CAVITY PROBLEM

The purpose of this section and the next one is, with the help of the resolution of two test problems, to;

- check both the zero-divergence of the velocity field and the definition of the vorticity at each time step.
- perform comparisons with results obtained by classical methods.

As a first test case we consider the well-known driven cavity problem (see Fig. 2) in the case of a Reynolds number Re equal to 400. The calculation were carried out on a 41×41 or a 61×61 grid. The reported results concern, as usual for this problem, the vorticity ω along the moving wall $y = 1$, the u-component of the velocity along the centerline $x = 0.5$, the streamlines pattern, and the isovorticity contours.

7.1. *Comparison of the Different Influence Matrix Techniques*

The purpose of this section is to show that the two influence matrix techniques that were described in Section 5

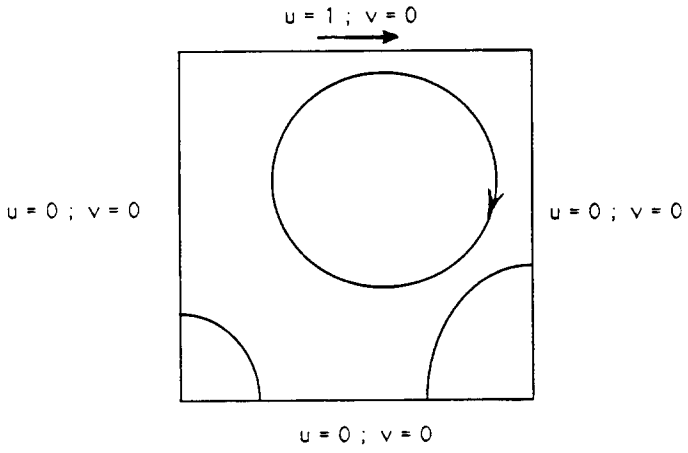

FIG. 2. The driven cavity: Sketch of the configuration.

TABLE I

l_2-Norm of the Differences

	$\Delta\omega$	Δu	Δv
(a)–(b)	1.3×10^{-12}	4.0×10^{-15}	2.5×10^{-15}
(b)–(c)	1.0×10^{-12}	2.0×10^{-16}	2.0×10^{-16}

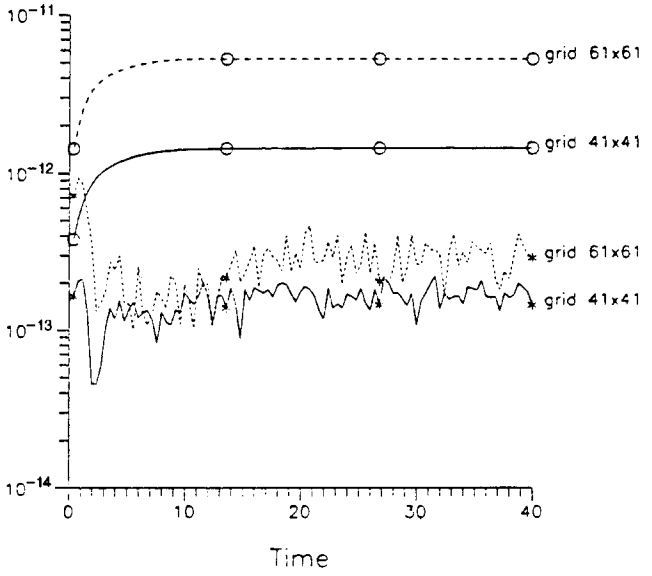

FIG. 3. Time evolution of: * max $|\nabla \cdot \mathbf{v}|$; ○ max $|\zeta - \omega|$.

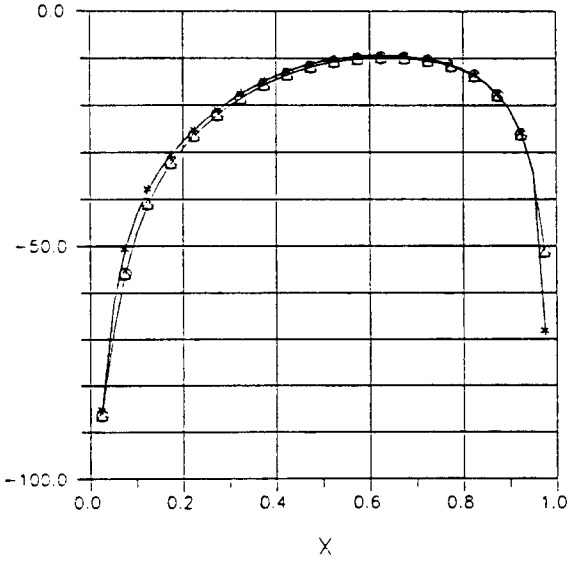

FIG. 4. Vorticity on the moving wall: * $\Psi - \omega$; △ case (a); ○ case (b).

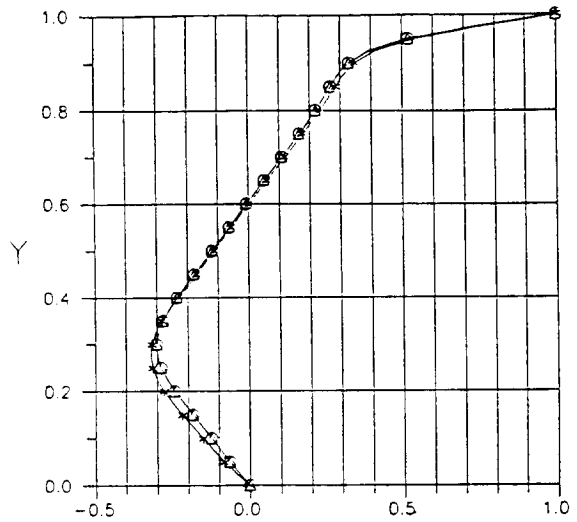

FIG. 5. u-component on the centerline $x = 0.5$: $* \ \Psi - \omega$; $\triangle$ case (a); $\bigcirc$ case (b).

give similar results within machine accuracy. Three cases are considered:

(a) $\zeta = \omega$ is satisfied at the N_Γ points of Γ.

(b) $\nabla \cdot \mathbf{v} = 0$ is satisfied at $N_\Gamma - 1$ points on Γ and $\zeta = \omega$ is satisfied at the center of the cavity.

(c) $\nabla \cdot \mathbf{v} = 0$ is satisfied at $N_\Gamma - 1$ points on Γ and $\zeta = \omega$ is satisfied at point (0.25, 0.25).

The l_2-norm of the differences $\Delta\omega$ on ω, Δu on u, and Δv on v are reported in Table I. These results clearly show that these techniques are equivalent, since the differences between the three cases vanish within machine accuracy.

7.2. *The Zero-Divergence and the Definition of the Vorticity*

The time evolutions of $\max |\nabla \cdot \mathbf{v}|$ and $\max |\zeta - \omega|$ are plotted on Fig. 3 for case (c) that has been defined previously and for two different grids: 41×41 and 61×61. It is clear that $\nabla \cdot \mathbf{v} = 0$ and $\zeta = \omega$ are satisfied within machine accuracy at each time step whatever the grid size, which shows the ability of the method to deal with real unsteady flows. The slight decrease in accuracy that is observed for the 61×61 grid, compared to the 41×41 one, is related to the use of a library routine to compute the inverse of the influence matrix **A**. Actually, the accuracy of these routines worsens with the increasing order of the matrix.

7.3. *Physical Features of the Flow*

Here we compare the results which have been obtained by means of the present $\mathbf{v} - \omega$ method with those that were computed by a finite differences $\Psi - \omega$ code developed by Daube and Ta Phuoc Loc [33]. This code uses a second-order scheme for the vorticity transport equation and a fourth-order scheme for the stream function equation.

The distribution of vorticity along the moving wall is plotted on Fig. 4 and the u-profile along the centerline $x = 0.5$ is plotted on Fig. 5. It is clear that the results are in very good agreement and that the observed differences can be related to the order of accuracy of the different schemes.

The streamlines (Fig. 6) and the isovorticity contours (Fig. 7) also show good agreement between the two codes in a satisfactory way the corner vortices that exist for this value of Re. The stream function Ψ was obtained in the case of the $\mathbf{v} - \omega$ formulation through the resolution of the Poisson equation $\nabla^2 \Psi = -\omega$.

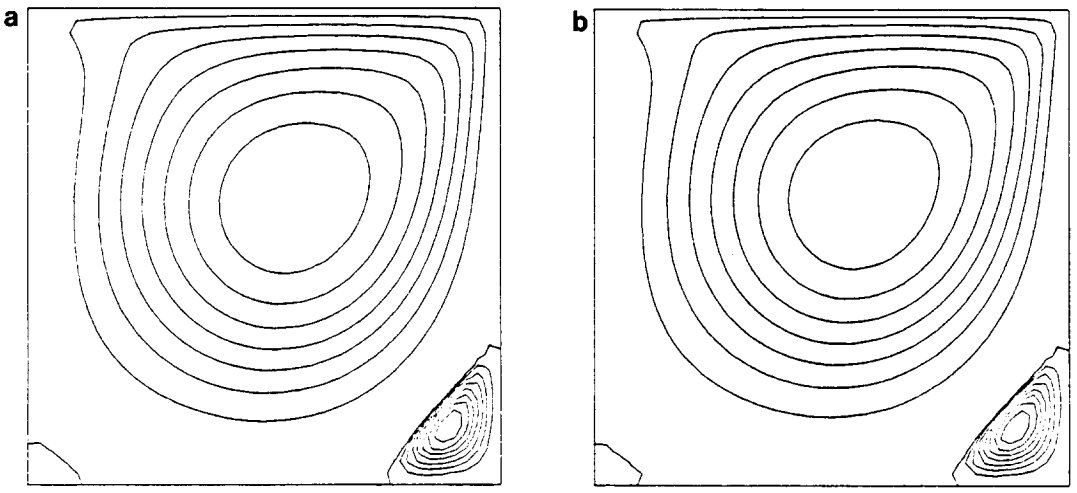

FIG. 6. Streamlines for Re = 400: (a) $\Psi - \omega$; (b) $\mathbf{v} - \omega$.

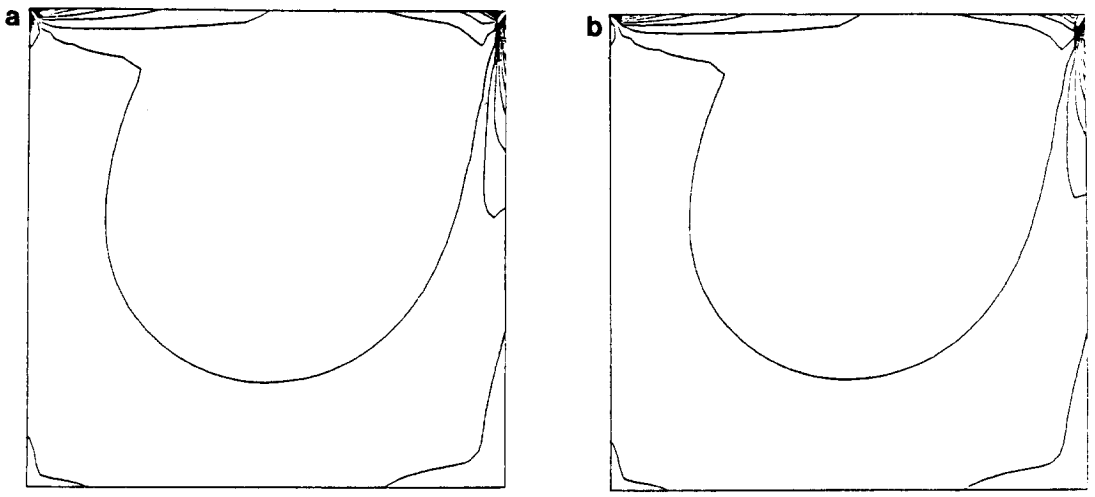

FIG. 7. Iso-vorticity contours for Re = 400: (a) $\Psi-\omega$; (b) $\mathbf{v}-\omega$.

8. AXISYMMETRIC FLOW IN A CLOSED CYLINDER

In this section, we check that the present method can be easily extended to axisymmetric flows.

8.1. *Statement of the Problem*

Let us consider a cylindrical tank (Fig. 8) of radius r_0 and of height H filled with an incompressible viscous fluid of kinematic viscosity ν. The motion of the fluid is due to the rotation at a constant angular velocity Ω of the lower lid. All the dependent and independent variables can be made dimensionless with respect to the length scale r_0, the velocity scale Ωr_0, and the time scale $1/\Omega$. Therefore the flow depends on two non-dimensional parameters: the rotational Reynolds number $\mathrm{Re}=\Omega r_0^2/\nu$ and the aspect ratio $h=H/r_0$.

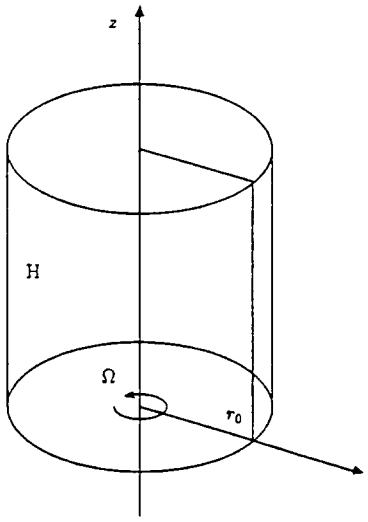

FIG. 8. The flow in a closed cylinder: Sketch of the configuration.

In cylindrical coordinates (r, θ, z), the radial, tangential, and axial components of the velocity are denoted by (u, v, w). We assume that the flow is axisymmetric. Thus, the Navier–Stokes equations read

$$\frac{\partial\omega}{\partial t}+\frac{\partial(u\omega)}{\partial r}+\frac{\partial(w\omega)}{\partial z}-\frac{\partial}{\partial z}\left(\frac{v^2}{r}\right)=\frac{1}{\mathrm{Re}}\left(\nabla^2-\frac{\mathrm{I}}{r^2}\right)\omega \tag{17}$$

$$\left(\nabla^2-\frac{\mathrm{I}}{r^2}\right)u=\frac{\partial\omega}{\partial z} \tag{18}$$

$$\nabla^2 w=-\frac{1}{r}\frac{\partial}{\partial r}(r\omega) \tag{19}$$

$$\frac{\partial v}{\partial t}+\frac{\partial(uv)}{\partial r}+\frac{\partial(wv)}{\partial z}+2\frac{uv}{r}=\frac{1}{\mathrm{Re}}\left(\nabla^2-\frac{\mathrm{I}}{r^2}\right)v, \tag{20}$$

where I is the identity operator and ∇^2 is the laplacian operator:

$$\nabla^2=\frac{\partial^2}{\partial z^2}+\frac{\partial^2}{\partial r^2}+\frac{1}{r}\frac{\partial}{\partial r}.$$

The continuity equation and the definition of the vorticity ω as the azimutal component of $\nabla\times\mathbf{v}$ read

$$\frac{\partial(ru)}{\partial r}+\frac{\partial(rw)}{\partial z}=0$$

$$\omega=\frac{\partial u}{\partial z}-\frac{\partial w}{\partial r}.$$

Boundary conditions. • **On the walls** the no-slip condition holds. For instance, on the rotating lid, this condition reads:

— $u(r, 0)=w(r, 0)=0, \forall r\in[0, 1]$

— $v(r, 0)=r, \forall r\in[0, 1]$.

• **On the rotation axis** symmetry considerations allow us to write:

$$-u(0, z) = v(0, z) = \omega(0, z) = 0, \forall z \in [0, h]$$

$$-\partial w/\partial r = 0, \forall z \in [0, h].$$

8.2. *Implementation of the Influence Matrix Technique*

The implementation of the technique is very similar to the cartesian case and the same temporal discretization can be used. It is easy to prove that it is sufficient to enforce either the continuity equation or the definition of the vorticity function ω on the solid boundary Γ because the relation $\zeta = \omega$ is automatically satisfied on the symmetry axis $r = 0$. Thus, the influence matrix is built exactly in the same manner by means of the discretized divergence or vorticity and the only points of the boundaries which are involved in this process are the points on the solid walls.

Therefore, one time step requires the resolution of two elliptic systems which are of the type,

$$\left(\left(\sigma + \frac{1}{r^2}\right) \mathrm{I} - \nabla^2\right) \omega = S_\omega$$

$$\left(\left(\sigma + \frac{1}{r^2}\right) \mathrm{I} - \nabla^2\right) v = S_v$$

$$\left(\nabla^2 - \frac{\mathrm{I}}{r^2}\right) u = \frac{\partial \omega}{\partial z}$$

$$\nabla^2 w = -\frac{1}{r} \frac{\partial}{\partial r} (r\omega),$$

with appropriate boundary conditions.

8.3. *Results for the steady case*

For this flow experimental data [34] as well as numerical results (35, 36] are available. They show, for instance, that for $\mathrm{Re} = 1850$ and $H/r_0 = 2$, the flow tends towards a steady state that exhibits two recirculation bubbles (one large and the other much smaller) on the symmetry axis. The streamline patterns found by Lugt [35], those computed by the $\Psi - \omega$ code mentioned in Section 7, and those computed from the vorticity field given by the present method are plotted on Fig. 9 and the agreement is very good.

The w-component along the symmetry axis is plotted on Fig. 10 and is compared to the profile obtained by the $\Psi - \omega$ code previously mentioned. The agreement between the two curves is almost perfect. They also compare very satisfactorily with the profile given by Lugt [35]. The locations where this velocity becomes positive indicate the recirculation bubbles.

Concerning the divergence and the definition of ω as the vorticity function, similar results to the cartesian case were found and are not reported here, i.e., the quantities $\nabla \cdot \mathbf{v}$ and $\zeta - \omega$ vanish within machine accuracy.

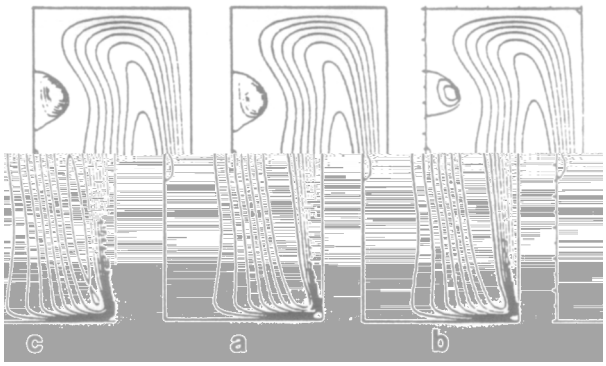

FIG. 9. Streamlines for $\mathrm{Re} = 1850$ and $H/r_0 = 2$: (a) $\Psi - \omega$; (b) $\mathbf{v} - \omega$; (c) from Lugt [33].

8.4. *The Unsteady Case*

As mentioned by Escudier [34] the flow becomes unsteady for values of Reynolds number larger than a critical value which depends on the aspect ratio of the tank. This problem was studied numerically by Daube and Sørensen [37] and by Lopez [36]. In particular, it is shown in [37] that in the case of an aspect ratio equal to 2, the flow undergoes a transition to a periodic flow with a frequency approximatively equal to 0.25 times the rotation frequency when the Reynolds number is larger than about 2600. This feature was also found with the present method.

Here we present a comparison with [37] in the case of an aspect ratio equal to 2 and $\mathrm{Re} = 2800$. Let A be the point of coordinates $(r = 0,\ z = 0.75h)$. The time evolutions of the axial component $w(A)$ computed by both methods are plotted in Fig. 11 and exhibit periodic behaviour which can also be seen on their power density spectrum (Fig. 12). The period Π of the oscillations is reported in Table II. We also

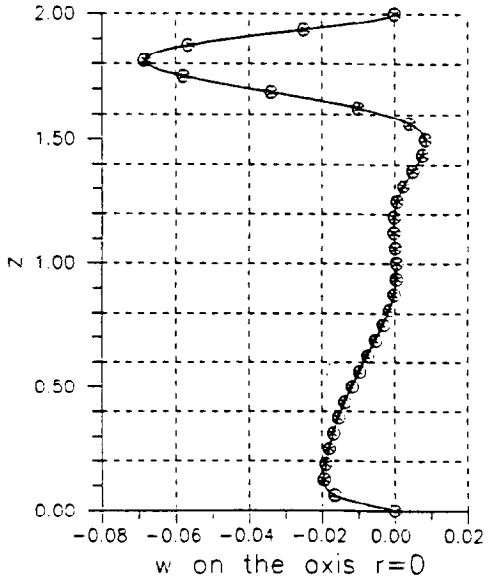

FIG. 10. w-profile on the symmetry axis: (a) $\Psi - \omega$; (b) $\mathbf{v} - \omega$.

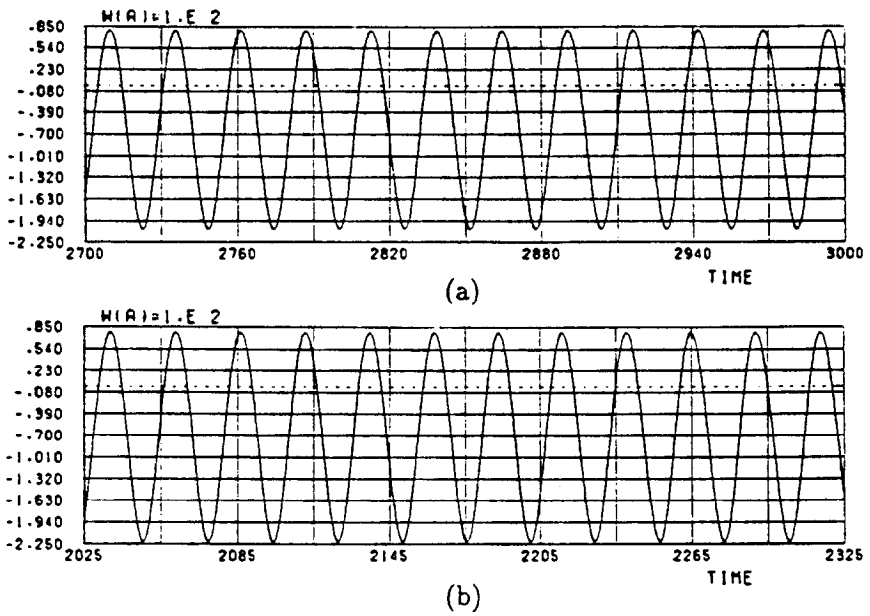

FIG. 11. Time evolution of $w(0, 3h/4)$ for Re = 2800 and $h = 2$: (a) $\Psi-\omega$; (b) $\mathrm{v}-\omega$.

give the period $\Pi^* = \Pi/2\pi$ expressed in the number of revolutions. In both methods, the time step Δt is equal to 0.05 and the observed difference between the periods is equal to 0.32, i.e., approximatively six times the time step. This difference may be significant and therefore the influence of the temporal discretization has to be checked.

In place of the ABCN scheme, another $\mathcal{O}(\Delta t^2)$ discretization was used which was proposed by Vanel *et al.* [25]. In this scheme, the time derivative at $(n+1)\,\Delta t$ is approximated by

$$\left(\frac{\partial f}{\partial t}\right)^{n+1} \simeq \frac{1}{2\Delta t}(3f^{n+1} - 4f^n + f^{n-1}).$$

Let CV be the convection terms. Using the notations of Section 3, we have

$$\sigma = \frac{3\mathrm{Re}}{2\Delta t};\ S^n = -\mathrm{Re}(2\mathrm{CV}^n - \mathrm{CV}^{n-1}).$$

With this new time discretization, the period was found to be equal to 25.56, i.e., within less than one time step from that obtained by the ABCN method. Hence the observed differences between the $\Psi-\omega$ results and the present ones are really significant and may be attributed to the different nature of the two methods.

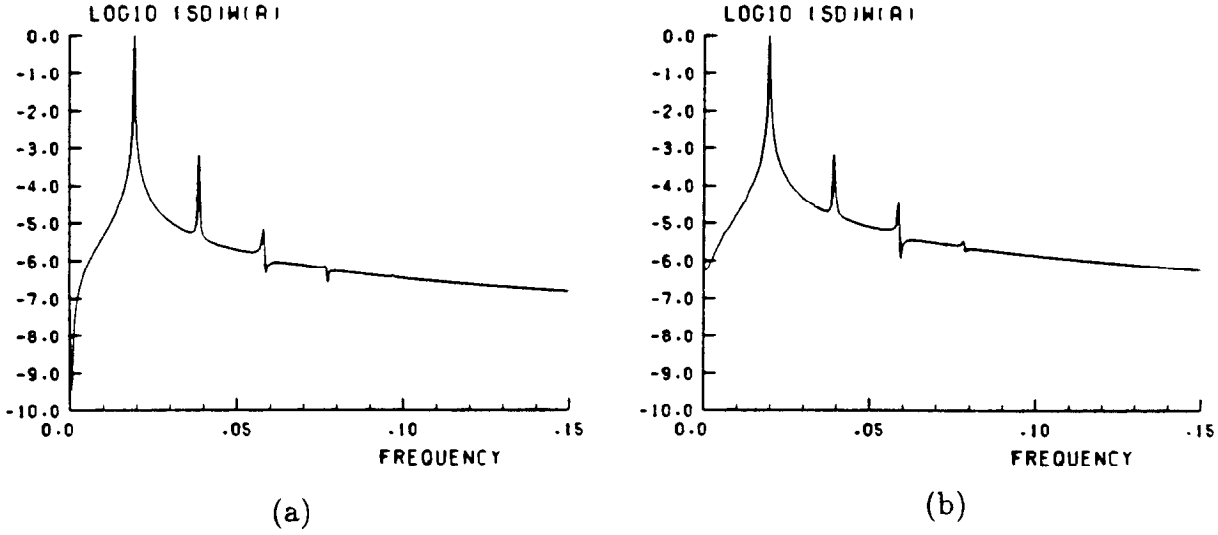

FIG. 12. Density power spectrum of the signal of Fig. 11: (a) $\Psi-\omega$; (b) $\mathrm{v}-\omega$.

TABLE II

Period of the Flow Oscillations for Re = 2800

Method	Π	Π^*
$\mathbf{v}-\omega$	25.52	4.06
$\Psi-\omega$	25.84	4.11

9. ON SOME DIFFICULTIES

Two main difficulties that arise during the course of this work have to be addressed briefly, although the basis of the vorticity–velocity formulation, especially corollaries (11) and (13) are not affected by them.

9.1. *Stability of the Scheme*

The temporal discretization is a semi-implicit one; i.e., the diffusion terms are treated implicitly, whereas the nonlinear terms are treated explicitly. Therefore this scheme has more severe stability criteria than purely implicit schemes. As an example, the resolution of the driven cavity flow at Re = 400 on a 41×41 grid, required a time step five times smaller than the time step needed for the implicit treatment of the $\Psi-\omega$ formulation ($\Delta t = 0.02$ instead of 0.1). Likewise, the time integration of the flow equations in the closed cylinder at Re = 1850 was carried out with a time step $\Delta t = 0.05$ in the case of the influence matrix technique, whereas a time step of 0.1 could be used in the case of the $\Psi-\omega$ formulation.

9.2. *On the Use of a Staggered Grid*

As many other authors, we found it necessary to use a staggered grid as described in Section 6. Every attempt to use a nonstaggered grid without special care in conjunction with the central differences led to either the blowing up of the computations or to nonphysical flows ($\nabla \cdot \mathbf{v} \neq 0$ and $\nabla \times \mathbf{v} \neq \omega \mathbf{k}$).

Basically, these difficulties are of the same nature as those that are encountered when dealing with the velocity–pressure formulation of the Navier–Stokes equations. They arise from the fact that the continuous operators and their discrete counterparts do not satisfy the same identities, especially when second-order operators are involved as composition of first-order ones.

Let us denote ∇_h the centered first difference operator on a nonstaggered grid. In the composition of two operators, e.g., $\nabla_h \cdot (\nabla_h)$ or $\nabla_h (\nabla_h \cdot)$, nodes (i, j), $(i \pm 2, j)$, and $(i, j \pm 2)$ are involved, whereas nodes (i, j), $(i \pm 1, j)$, and $(i, j \pm 1)$ are involved in the usual discretization of the laplacian ∇_h^2. That means that with such a discretization, there is no discrete counterpart of the continuous vector identity $\nabla \cdot \nabla f = \nabla^2 f$, i.e., $\nabla_h \cdot (\nabla_h f) \neq \nabla_h^2 f$. This fact is the basis of the odd–even decoupling for the pressure in primitive variables formulation. In our case, the proofs of corollaries (3) and (6) are based upon the extensive use of the vector identity (6), which defined the laplacian vector, and of classical vector analysis relations.

It is therefore necessary to use a grid and discrete operators (curl, gradient, and laplacian) so that an identity analogous to (6) is satisfied in addition to the usual relations $\nabla_h \cdot (\nabla_h \times \mathbf{v}) = 0$ and $\nabla_h \times (\nabla_h f) = 0$. If doing so, the discretized version of problem (8) is fully equivalent to the discretized version of problem (11) or (13). This means, for instance, that if the definition of the discrete vorticity is satisfied on the boundary, it will also be true at the interior nodes. The use of a MAC grid, in conjunction with the discrete operators defined in Section 6, is a well-known straightforward way to ensure that the discrete analogue of the vector identity (6) is satisfied. This is the reason why we chose this kind of grid in this work. However, it is clear that this restriction will have to be overcome if we want to extend this work to configurations involving curvilinear coordinates and/or nonuniform grids. Moreover, the difficulties will be obviously worse in real 3D flows.

These problems have already been considered by many people in the case of the formulation of primitive variables. The papers by Rhie and Chow [38], Schneider and Raw [40], Strikwerda [39], and more recently by Armfield [41] are of particular interest and the collocated schemes that they designed are more and more widely used. A similar work has not yet been done in the context of the velocity–vorticity formulation. The theoretical concepts—as the symbol of an operator (see [39, 41])—that are underlying these schemes are likely to be used to design nonstaggered schemes which would preserve the desirable features of this work, i.e., the zero divergence and the definition of the vorticity as the curl of the velocity.

CONCLUSIONS

In this paper we have shown that it is possible to solve the 2D incompressible Navier–Stokes equations written in velocity–vorticity formulation by means of an influence matrix technique. At each time step, a strong coupling between the vorticity and the velocity field is enforced and the continuity equation, as well as the definition of the vorticity, are satisfied within machine accuracy. Therefore the present method allows us to study accurately and efficiently unsteady flows, as was shown for the two test cases considered.

Beyond this fact, we want to emphasize the necessity to obtain, *at each time step*, either a correct definition of ω as the vorticity of the velocity field $\mathbf{v}$ or the vanishing of the divergence on the solid boundaries. Actually, it is believed that this is the crucial point when using the $\mathbf{v}-\omega$ formulation, whatever the numerical technique that is used.

The main question that arises now is the extension of this technique to 3D flows. In addition to the difficulties which were previously mentioned concerning the use of a MAC grid, the tractability of an influence matrix has to be considered because of its large size. This difficulty may be partly avoided for flows with one direction of periodicity. In this case, the use of Fourier series expansions in this direction avoids the use of a too-large influence matrix that actually reduces to a sequence of N_k 2D influence matrices that can be "easily" inverted, where N_k is the number of Fourier modes that are considered. Another important point that has to be noted is that the boundary conditions that have to be enforced by means of this influence matrix are not so "obvious" as in the 2D case [14]. In particular, special care has to be taken in order to ensure that the vorticity vector field ω is solenoïdal.

ACKNOWLEDGMENTS

Dr. P. LeQuéré and Professor S. Korpela are gratefuly acknowledged for very helpful discussions during the course of this work. The CPU time on the Fujitsu VP200 at CIRCE was provided by the "Direction Scientifique du Département SPI du CNRS."

REFERENCES

1. C. G. Speziale, *J. Comput. Phys.* **73**, 476 (1987).
2. G. Guevremont, W. G. Habashi, and M. M. Hafez, *Int. J. Num. Methods Fluids* **10**, 461 (1990).
3. H. Fasel, *J. Fluid Mech.* **78**, 355 (1976).
4. S. C. R. Dennis, D. B. Ingham, and R. N. Cook, *J. Comput. Phys.* **33**, 325 (1979).
5. G. A. Osswald, K. N. Ghia, and U. Ghia, in *Proceedings, 11th International Conference on Numerical Methods in Fluid Dynamics, Williamsburg, VA, 1988*, edited by D. L. Dwoyer *et al.* (Springer-Verlag, Berlin, 1989), p. 454.
6. T. B. Gatski, C. E. Grosch, and M. E. Rose, *J. Comput. Phys.* **48**, 1 (1982).
7. T. B. Gatski, C. E. Grosch, and M. E. Rose, *J. Comput. Phys.* **82**, 298 (1989).
8. P. Orlandi, *Comput. Fluids* **15**, 137 (1987).
9. A. Toumi and T. Phuoc Loc, in *Proceedings, 5th International Conference on Numerical Methods in Laminar and Turbulent Flows, Montreal, Canada, 1987*, edited by C. Taylor *et al.* (Pineridge Press, Swansea, UK, 1987), p. 595.
10. G. H. Cottet, in *Mathematical Aspects of Vortex Methods*, edited by R. E. Caflish (SIAM, Providence, RI, 1988), p. 129.
11. W. Labidi and T. Phuoc Loc, in *Proceedings, 11th International Conference on Numerical Methods in Fluids Dynamics, Williamsburg, VA*, edited by D. L. Dwoyer *et al.* (Springer-Verlag, Berlin, 1989), p. 354.
12. B. Farouk and T. Fugesi, *Int. J. Num. Methods Fluids* **5**, 1017 (1985).
13. F. Stella and G. Guj, *Int. J. Num. Methods Fluids* **9**, 1285 (1989).
14. O. Daube, J. L. Guermond, and A. Sellier, *C. R. Acad. Sci. Paris Sér. II* **313**, 377 (1991).
15. R. Hockney, *Methods Comput. Phys.* **9**, 135 (1970).
16. W. Proskurowski and O. Widlund, *Math. Comput.* **30**, 433 (1976).
17. W. Proskurowski, *ACM Trans. Math. Software* **5**, 36 (1979).
18. A. Pares-Sierra and G. K. Vallis, *J. Comput. Phys.* **82**, 398 (1989).
19. L. Kleiser and U. Schumann, in *Proceedings, 3rd GAMM–Conference on Numerical Methods in Fluid Mechanics, Köln, Germany, 1979*, edited by E. H. Hirschel, Notes on Num. Fluid Mech. (Vieweg, Wiesbaden, 1980), p. 165.
20. P. Le Quéré and T. Alziary de Roquefort, *C.R. Acad. Sci. Paris, Sér. II* **294**, 941 (1982).
21. P. Le Quéré and T. Alziary de Roquefort, *J. Comput. Phys.* **57**, 210 (1985).
22. L. Tuckermann, *J. Comput. Phys.* **80**, 403 (1989).
23. S. C. R. Dennis and L. Quartapelle, *J. Comput. Phys.* **52**, 448 (1983).
24. L. Tuckermann, Ph.D. thesis, MIT, Cambridge, MA, 1983 (unpublished).
25. J. M. Vanel, R. Peyret, and P. Bontoux, in *Proceedings, International Conference on Numerical Methods for Fluids Dynamics, Reading, UK, 1985*, edited by K. W. Morton and M. J. Baines (Clarendon Press, New York, 1986), p. 463.
26. L. Quartapelle and M. Napolitano, *J. Comput. Phys.* **62**, 340 (1986).
27. L. Quartapelle and A. Muzzio, in *Proceedings, International Symposium on Computational Fluid Dynamics, Sydney, Australia, 1987*, edited by G. De Vahl Davis and C. Fletcher (North-Holland, Amsterdam, 1988), p. 609.
28. L. Quartapelle, in *Proceedings, International Conference for Computational Methods in Flow Analysis, Okayama, Japan, 1988*, p. 337.
29. R. Glowinski and O. Pironneau, *SIAM Rev.* **21**, 167 (1979).
30. R. Peyret and T. D. Taylor, *Computational Methods for Fluid Flows* (Springer-Verlag, New York, 1983), p. 151.
31. R. W. Hockney, *J. Assoc. Comput. Mach.* **12**, 95 (1965).
32. D. Fischer, G. Golub, O. Hald, C. Leiva, and O. Widlund, *Math. Comput.* **28**, 349 (1974).
33. O. Daube and T. Phuoc Loc, *J. Méc.* **17**, 651 (1978).
34. M. P. Escudier, *Exp. Fluids* **2**, 189 (1984).
35. H. J. Lugt and M. Abboud, *J. Fluid Mech.* **179**, 179 (1987).
36. J. M. Lopez, *J. Fluid Mech.* **221**, 533 (1990).
37. O. Daube and J. N. Sørensen, *C.R. Acad. Sci. Paris Sér. II* **308**, 463 (1989).
38. C. M. Rhie and W. L. Chow, *AIAA J.* **21**, 1525 (1983).
39. J. C. Strikwerda, *SIAM J. Sci. Stat. Comput.* **5**, 56 (1984).
40. G. Schneider and M. Raw, *Numer. Heat Transf.* **11**, 363 (1987).
41. S. W. Armfield, *Comput. & Fluids* **20**, 1 (1991).